

# Industrial Scale Direct Liquefaction of *E. globulus* Biomass

Irina Fernandes <sup>1</sup>, Maria Joana Neiva Correia <sup>1</sup> , José Condeço <sup>1</sup> , Duarte M. Cecílio <sup>1,2</sup>, João Bordado <sup>1</sup> and Margarida Mateus <sup>1,2,\*</sup> 

- <sup>1</sup> CERENA, Centro de Recursos Naturais e Ambiente, Departamento de Engenharia Química, Instituto Superior Técnico, Universidade de Lisboa, Av. Rovisco Pais, 1049-001 Lisboa, Portugal; irina.fernandes@tecnico.ulisboa.pt (I.F.); qjnc@tecnico.ulisboa.pt (M.J.N.C.); jose.condeco@tecnico.ulisboa.pt (J.C.); duarte.cecilio@secil.pt (D.M.C.); jcbordado@tecnico.ulisboa.pt (J.B.)
- <sup>2</sup> Secil S.A., Fábrica Secil-Outão, 2901-864 Setúbal, Portugal
- \* Correspondence: margarida.mateus@tecnico.ulisboa.pt

**Abstract:** This work presents the study of *Eucalyptus globulus* bark and sawdust direct liquefaction. Laboratory scale experiments were carried out to assess the impact of several variables on the reaction yield and the sugar content of the bio-oil. These variables were the biomass type and concentration, the solvent, and the reaction time. The results show that *E. globulus* sawdust presented the highest yields (>95%), but the highest sugar content after water extraction was obtained for *E. globulus* bark (~5.5% vs. 1.2% for sawdust). Simultaneously, industrial-scale tests were carried out at the ENERGREEN pilot plant using the same reaction variables, which resulted in reaction yields of nearly 100%. The reagents and raw materials used, as well as the products obtained (bio-oil, reaction condensates, polyols, and sugar phases) were characterized by elemental analysis, infrared spectroscopy, thermogravimetry, and high-performance liquid chromatography with mass spectrometry. The heating value of the bio-oils is higher than the original biomass (higher heating value of *E. globulus* sawdust bio-oil 29 MJ/kg vs. 19.5 MJ/kg of the original *E. globulus* sawdust). The analyses of the bio-oils allowed us to identify the presence of high-added-value compounds, such as levulinic acid and furfural. Finally, a study of the accelerated aging of liquefied biomass showed that the biofuel density increases from 1.35 to 1.44 kg/dm<sup>3</sup> after 7 days of storage due to the occurrence of repolymerization reactions.



**Citation:** Fernandes, I.; Correia, M.J.N.; Condeço, J.; Cecílio, D.M.; Bordado, J.; Mateus, M. Industrial Scale Direct Liquefaction of *E. globulus* Biomass. *Catalysts* **2023**, *13*, 1379. <https://doi.org/10.3390/catal13101379>

Academic Editor: Claudia Carlucci

Received: 6 August 2023

Revised: 14 September 2023

Accepted: 28 September 2023

Published: 19 October 2023



**Copyright:** © 2023 by the authors. Licensee MDPI, Basel, Switzerland. This article is an open access article distributed under the terms and conditions of the Creative Commons Attribution (CC BY) license (<https://creativecommons.org/licenses/by/4.0/>).

**Keywords:** ENERGREEN; biomass liquefaction; pilot scale; bio-oils; sugar extraction; stabilization

## 1. Introduction

Fossil fuels are the largest source of energy currently in use due to their abundance and relatively low cost. However, apart from being non-renewable sources of energy, fossil fuels have several negative environmental impacts, like global warming and air pollution. These negative impacts, together with the increase in the demand for energy sources, partially due to the huge increase in the world's population [1], have been the drivers for the increasing interest in renewable energy sources, namely biomass.

Biomass is considered the source of renewable energy with the greatest potential to bridge the energy needs of modern societies and includes forest residues (lignocellulosic biomass) and industrial or domestic organic wastes [2,3]. Of these, lignocellulosic biomass is one of the most promising renewable energy resources and can be used by direct combustion or other efficient and competitive alternatives, such as thermochemical conversion, fermentation for bioethanol production, or anaerobic digestion for biogas production [4].

Lignocellulosic biomass is formed by three main constituents: cellulose, hemicellulose, and lignin [5,6]. Cellulose, with the molecular formula of (C<sub>6</sub>H<sub>10</sub>O<sub>5</sub>)<sub>n</sub>, is a linear polymer of glucose units connected through glycosidic bonds and can have crystalline or amorphous structures [7,8]. Crystalline cellulose is not depolymerizable at low temperatures [8,9]. Cellulose represents between 40 and 60% of the biomass composition. Hemicellulose,

which constitutes between 20 and 40% of the biomass, is an amorphous heteropolymer formed by monosaccharide units of hexoses, such as glucose, mannose, and galactose, and pentoses, such as xylose and arabinose; hemicellulose chains are easily hydrolyzed due to their branched structure and low molecular weight [6–8]. Finally, lignin, which can represent between 10 and 25% of the biomass composition, is a highly branched amorphous biopolymer that is mainly composed of phenolic alcohols, such as p-coumaryl, synapil, and coniferyl alcohols; the high degree of branching of lignin leads to a three-dimensional network, which is difficult to chemically depolymerize [9].

There are a lot of publications about biomass direct liquefaction. Recently, the work of Fernandes et al. [10] describes the optimization of the liquefaction of *E. globulus* sawdust, namely the reaction time, catalyst concentration, temperature, and biomass-to-solvent ratio. The optimized conditions led to a maximum conversion rate of 96%. Characterization of the bio-oil was performed using FTIR-ATR, elemental analysis, and thermogravimetry. The characterization confirmed the presence of biomass-based compounds in the bio-oil. Paulo et al. [11] studied the acid-catalyzed liquefaction of eight short rotation coppice (SRC) poplar clones, aiming to convert the biomass into bio-oil at mild temperatures and ambient pressure. The produced bio-oil had a carbon content of 65%, oxygen content of 26%, and hydrogen content of 8.7%, with an average higher heating value (HHV) of 30.5 MJ/kg. The van Krevelen diagram demonstrated that the bio-oils exhibited chemical compatibility with liquid fossil fuels, like diesel or gasoline. The FTIR analysis indicated the substantial chemical conversion of the raw biomass, with evidence of the presence of lignin and hemicellulose depolymerization derivatives in the bio-oil. TGA in the nitrogen atmosphere showed that the bio-oils were more volatile than the fresh feedstock, requiring lower peaking temperatures for their vaporization and decomposition. Comparing the bio-oil with the biomass, the atomic ratios of H/C increase and O/C decrease, indicating that the bio-oil has better fuel characteristics. Overall, the liquefaction results confirmed the potential of SRC poplar biomasses for energy and chemical production.

Silva et al. [12] quantified the sugars present in the aqueous extract of the bio-oil produced by the thermochemical liquefaction of *E. globulus*. The investigation employed HPLC-RID, a fast, economical, and accurate analytical method, to identify and quantify the sugars in the aqueous extracts. HSQC-NMR and FTIR-ATR analyses confirmed the presence of carbohydrates in the aqueous extracts. The main sugars identified were fructose (36.58%), glucose (33.33%), sucrose (15.14%), trehalose (4.82%), and xylose (10.13%).

#### *Liquefaction Process*

The thermochemical conversion of biomass can be divided into three different processes: gasification, pyrolysis, and liquefaction. Liquefaction can be carried out in different conditions at high temperatures (>200 °C) and pressures, such as in hydrothermal upgrading, HTU, or at moderated temperatures (100–250 °C) and atmospheric pressure in the presence of solvent and a catalyst, such as in direct liquefaction studied in this work [4,13]. In this process, biomass chains are broken into smaller molecules by a reaction with a solvent at temperatures between 150 and 250 °C and atmospheric pressure. Usually, a single or a mixture of polyhydric alcohols is used as a solvent [14]. Biomass liquefaction is a significantly complex process due to the large variety of reactions that occur simultaneously, like the solvolysis between the biomass and the solvent, depolymerization of the major components of biomass, repolymerization, decarboxylation reactions, degradation reactions of oxygenated compounds in the presence of hydrogen, etc. [15,16]. The occurrence of several of these reactions is strongly influenced by the operating conditions (temperature, biomass type and composition, solvent, catalyst, etc.) [4,13]. Of these, biomass composition and temperature are important variables. In fact, a low reaction temperature will lead to low liquefaction yields but high temperatures can lead to repolymerization reactions [16–18]. On the other hand, the relative composition of cellulose, hemicellulose, and lignin greatly influences the behavior of the biomass during liquefaction. In fact, the higher the amount of lignin, the lower the conversion into bio-oil [4,18,19]. Actually, when lignin is thermally

decomposed at high temperatures, it forms free radicals of phenol that can react through re-polymerization and condensation reactions to produce solid residues [18]. Crystalline cellulose, with a more ordered structure, also presents low liquefaction rates [20].

In this work, the study of *E. globulus* bark and sawdust biomass upgrading via direct liquefaction, carried out at laboratory and pilot scales, to yield a liquid biofuel with improved heating value and shelf life is presented.

## 2. Results

### 2.1. Characterization of Biomass Feedstocks

The elemental composition and higher heating value (HHV) of the biomass samples are presented in Table 1. As seen, sawdust has a higher HHV and a lower moisture content, which will result in lower energy consumption for water evaporation during liquefaction. It is also observed that the *E. globulus* bark has a higher ash content that will result in a higher content of solids after the reaction.

**Table 1.** Biomass elemental composition (*w:w*) and HHV.

Biomass Analysis	<i>E. globulus</i> Bark	<i>E. globulus</i> Sawdust
Weight loss at 105 °C (%)	53.4	44.4
Ash (%)	6.4	1.7
C (%) *	46.0	49.3
H (%) *	5.3	5.7
N (%) *	1.2	1.0
S (%) *	0.1	0.1
Cl (%) *	0.2	0.1
O (%) **	47.2	43.8
HHV (kJ/kg)	17,730	19,460

\* daf—dry ash-free basis; \*\* oxygen determined by difference; mass percentages.

The FTIR spectra of the two biomass samples, together with the spectra of cellulose, hemicellulose, and lignin standards, are presented in Figure 1.

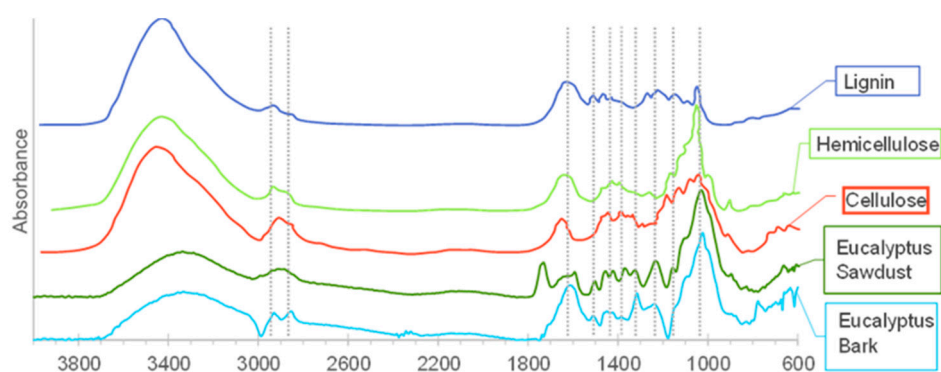


**Figure 1.** FTIR spectra of the biomasses and cellulose, hemicellulose, and lignin standards.

By observing the FTIR spectra of the biomass samples and comparing them with the standard spectra of cellulose, hemicellulose, and lignin presented by Galletti et al. [21], it is possible to attribute the different peaks to each compound. Thus, the spectra of all samples display a prominent band within the range of 3500–3200  $\text{cm}^{-1}$ , which can be attributed to the stretching vibration of hydroxyl groups. This intense signal in all biomasses indicates the presence of abundant hydroxyl functional groups due to, for example, moisture. *E. globulus* bark has peaks in the range of 2930 and 2850  $\text{cm}^{-1}$  of aliphatic C-H stretching [14], which is characteristic of lignin and hemicellulose, whereas at these wavenumbers, sawdust has a single peak observed for cellulose. Another prominent peak in the spectrum of *E. globulus* bark and of the three biopolymers occurs at 1730–1620  $\text{cm}^{-1}$  and is due to the

C-O stretching of hemicellulose and lignin and the C-C stretching of the lignin aromatic rings [14]. Peaks at  $1510\text{ cm}^{-1}$  and  $1320\text{ cm}^{-1}$  are found in the spectra of both biomasses and stand out, respectively, in the lignin and cellulose spectra. Finally, it is worth mentioning that the peak at  $1025\text{ cm}^{-1}$  is seen in all spectra but has greater intensity in the spectrum of hemicellulose.

The TGA and DTG curves of the biomass samples and the standards are presented in Figure 2. The TGA of *E. globulus* bark shows the first weight loss of 55.9% between  $25\text{ }^{\circ}\text{C}$  and  $140\text{ }^{\circ}\text{C}$  or, more precisely from the DTG curve, at  $95.4\text{ }^{\circ}\text{C}$ . This mass loss is due to moisture evaporation. The second plateau, with a mass loss of 5.1%, occurs between  $140$  and  $300\text{ }^{\circ}\text{C}$ ; the comparison with the standards allows us to conclude that this mass loss corresponds to the degradation of hemicellulose. The third plateau, corresponding to a mass loss of 20.0%, appears between  $300$  and  $420\text{ }^{\circ}\text{C}$ , and is the loss peak at  $349.5\text{ }^{\circ}\text{C}$ , which corresponds to cellulose degradation. Finally, the fourth plateau, with a mass loss of 5.6%, is due to lignin degradation that occurs throughout the test. The solid residue determined by difference corresponds to 13.4%. It is worth noting that the results for *E. globulus* dust (not presented) were similar with some deviations in the pick temperatures.

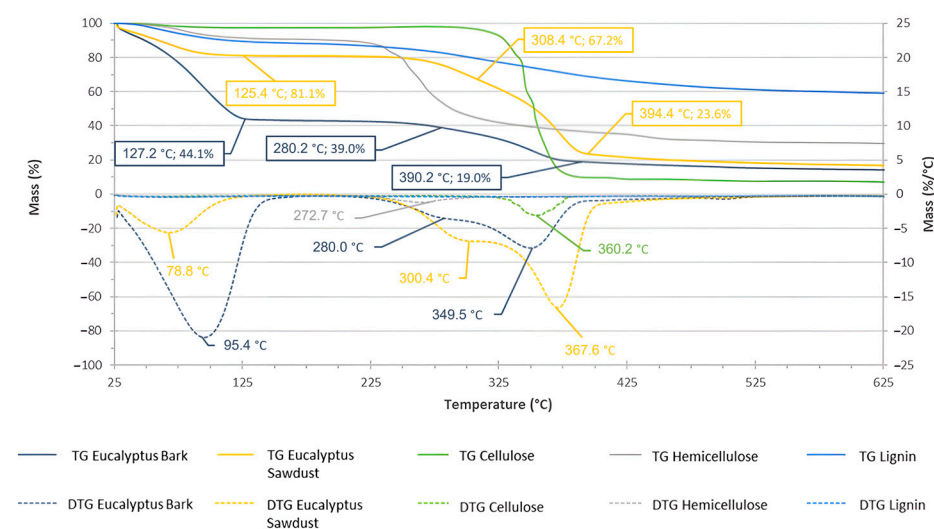


**Figure 2.** TGA (continuous line) and DTG (dotted line) analyses of the biomasses and standards.

The TGA results allowed us to establish the relative composition (dry basis) in the three biopolymers of the two biomass samples (Table 2). As shown, *E. globulus* sawdust presents a higher content of hemicellulose and a lower content of lignin, which indicates that it should be easily liquified.

**Table 2.** Biomass dry basis composition based on TGA (under  $\text{N}_2$  atmosphere).

Composition	<i>E. globulus</i> Bark	<i>E. globulus</i> Sawdust
Hemicellulose	11.6%	17.1%
Cellulose	45.3%	53.8%
Lignin	12.7%	10.5%
Residue	30.4%	18.6%

## 2.2. Laboratory Scale Liquefaction

### Semi-Batch Liquefaction Tests

The *E. globulus* bark and sawdust liquefaction were performed in semi-batch mode using the conditions reported in Section 3.

Biomass additions were made over time to mimic the industrial pilot scale reaction. Figure 3 shows the observed decrease in the solvent mass percentage as biomass is introduced in the reactor, while the catalyst concentration remains between 2% and 3%.

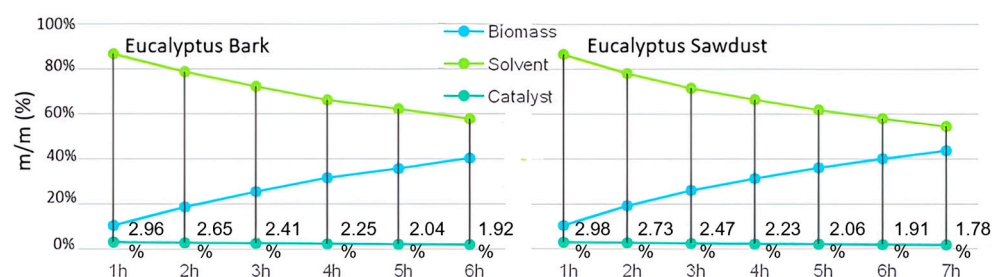


**Figure 3.** Biomass, solvent, and catalyst contents in the liquefaction of *E. globulus* bark and sawdust with sequential biomass additions.

It is worth noting that the reaction was stopped after 6 h of bark addition and 7 h of sawdust addition since the reaction medium became very viscous [22]. The analysis of samples of the reaction mixture collected before each biomass addition allowed us to estimate the conversion of the biomass into bio-oil, which was higher than 90%.

After liquefaction and sugar extraction with the reaction condensates, the drying of the aqueous phases at 60 °C until constant weight allows us to determine the sugar content. For bark, the mass of sugars recovered was 5.8% of the initial aqueous phase, whereas for sawdust, this value was 1.2% [23].

The bio-oils and the hydrophobic fractions produced after sugar extraction, called polyols, were analyzed. As seen in Table 3, both phases have higher calorific values than the original biomasses (Table 1). Notably, the calorific value decreased from the liquefied product to the polyols phase, which can be attributed to the formation of a microemulsion with water during sugar extraction. In fact, the weight loss at 105 °C verified for *E. globulus* bark polyols was 55.9% higher than in the bio-oil. This increase was less pronounced for sawdust (6.8%) because the liquefied product already has a high water content.

**Table 3.** Elemental analysis, weight loss at 105 °C, and calorific values of the liquefied product and polyols of *E. globulus* bark and sawdust.

Analysis	<i>E. globulus</i> Bark		<i>E. globulus</i> Sawdust	
	Bio-Oil	Polyols	Bio-Oil	Polyols
Weight loss at 105 °C (%)	7.0	62.9	46.8	53.6
C (%) *	62.4	45.2	65.3	56.3
H (%) *	11.7	9.3	9.7	9.8
N (%) *	1.8	1.2	1.3	1.2
S (%) *	0.3	0.1	0.4	0.3
O (%) **	23.8	44.2	23.3	32.4
HHV (kJ/kg)	32,915	21,585	32,405	27,685

\* daf—dry ash-free basis; \*\* oxygen determined by difference; mass %.

FTIR spectra of samples of the liquefied product taken before each addition of *E. globulus* bark to the reactor were also collected. As shown in Figure 4, all liquefied products exhibited the characteristic peaks of the 2EH spectrum. On the other hand, the peaks at 1750 cm<sup>-1</sup> and 1235 cm<sup>-1</sup> increased in intensity with the number of biomass increments. These peaks correspond to C=O bonds, which are characteristic of ketone or aldehyde functional groups, and COOH bonds, which are characteristic of carboxylic groups [12]. The increase in these peaks' intensity with the reaction time can be attributed to cellulose depolymerization into levulinic acid and furfural or an increase in hemicellulose content due to the addition of biomass [24,25]. The elongated peak in the range of 3300 cm<sup>-1</sup>, representing OH groups, is typically associated with moisture [26].

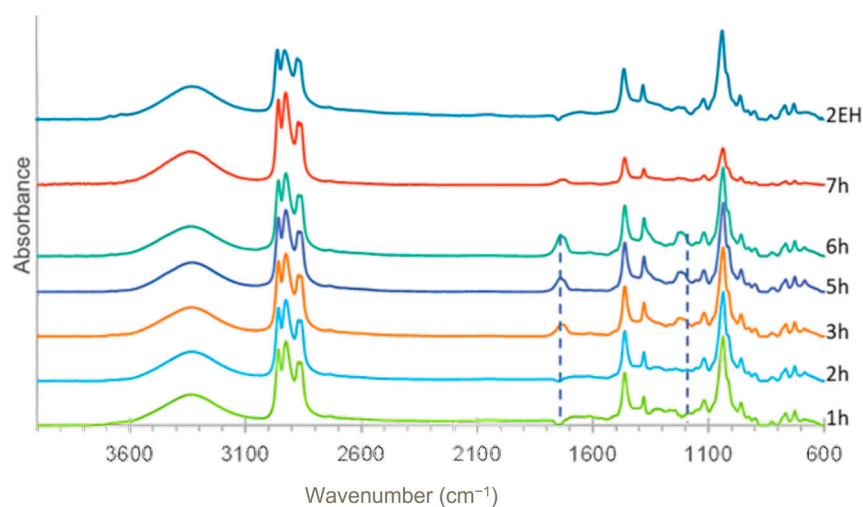


**Figure 4.** FTIR spectra of the liquefied product before each incremental addition of *E. globulus* bark.

Figure 5 displays the FTIR spectra of polyols and pure and condensed solvents. As seen, the polyols exhibit peaks corresponding to 2EH, particularly in the 3000–2800  $\text{cm}^{-1}$  range. The peaks at 1790  $\text{cm}^{-1}$  and 1685  $\text{cm}^{-1}$  in the polyols spectrum are characteristic of C=O bonds [22]. These peaks indicate the presence of soluble fragments produced during depolymerization reactions, such as levulinic acid, lactic acid, and/or furfural [24,25]. However, these peaks can also be attributed to the presence of partially depolymerized hemicellulose and lignin [26]. The band at 1610  $\text{cm}^{-1}$ , due to CH<sub>2</sub> bonds, can also indicate the presence of cellulose and hemicellulose polymers [12]. Finally, the peaks at 1575, 1465, 1213, 1138, 877, and 839  $\text{cm}^{-1}$  are observed in the spectra of pure and condensed solvents.

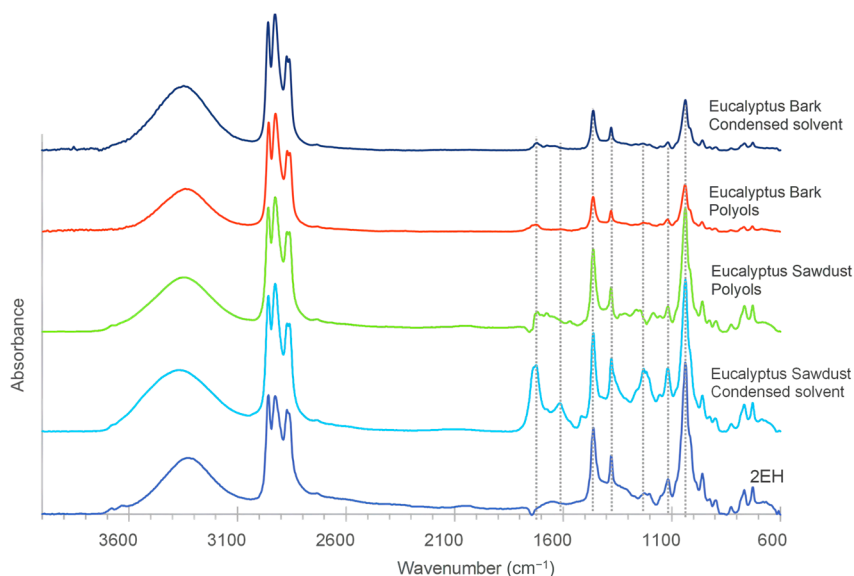


**Figure 5.** FTIR spectra of the polyols and pure and condensed solvent from the liquefaction reaction of *E. globulus* bark and sawdust.

### 2.3. Pilot Scale Liquefaction Tests

In addition to the laboratory experiments, several tests were conducted in an industrial liquefaction pilot facility using laboratory-established conditions. The main objective of the ENERGREEN pilot plant is to produce a clean and sustainable biofuel with a high calorific value to be used in the cement kiln. Therefore, the reaction products obtained after the liquefaction of *E. globulus* sawdust, namely the liquefied biomass, the polyols,

the condensates, the extraction waters, and the sugars resulting from the reactions, were analyzed using the previously described techniques.

### 2.3.1. Characterization of the Bio-Oils

Table 4 presents the elemental analysis, calorific value, density, and viscosity of the bio-oil produced in *E. globulus* sawdust liquefaction.

**Table 4.** Elemental analysis, weight loss at 105 °C, calorific value, and density of bio-oils produced in the first liquefaction reaction. (Solvent: 2EH).

Reaction Time (h)	24 h	48 h
Weight loss at 105 °C % (m/m)	-	40.0
C (%) *	70.3	44.1
H (%) *	12.9	11.1
N (%) *	2.3	1.1
S (%) *	0.3	0.9
O (%) **	14.2	42.8
HHV (kJ/kg)	38,790	22,880
LHV (kJ/kg)	36,065	20,525
Density (kg/dm <sup>3</sup> )	0.80 (25 °C)	0.92 (25 °C)

\* daf—dry ash-free basis; \*\* oxygen determined by difference; %-mass percentage.

The results presented in Table 4 reveal a slight increase in density with time and biomass additions. Regarding the calorific value of the liquefaction products, it is found that it is higher than the initial biomass (HHV = 19,530 kJ/kg), indicating that the bio-oil is of higher value. The high value of the weight loss at 105 °C after 48 h of reaction (40%) is certainly correlated with 2EH water azeotrope. Nevertheless, the average water content, determined by the Karl Fisher method, of the liquefied samples at the end of the reaction was only 2.1%.

Previous work showed that the best liquefaction conversion was obtained when a mixture of 1:1 of DEG and 2-EH was used as solvents [4]. Therefore, two tests were carried out using this mixture of solvents (Tables 5 and 6).

Comparing the values presented in Tables 4–6, it is possible to conclude that the bio-oils produced in these three liquefactions were similar. Furthermore, since DEG is denser and more viscous than 2EH, the density of the liquefied products obtained using the mixture of solvents is higher than when EH was used alone. Again, the high weight loss at 105 °C of the different samples in Table 6 is also due to the 2EH water azeotrope. However, as shown in Tables 5 and 6, the water content of the bio-oils was only 9.2% and 2.1%, respectively.

**Table 5.** Elemental analysis, weight loss at 105 °C, moisture content, calorific value, and density of the liquefied product produced in the second liquefaction reaction. (Solvent: 2EH and DEG 1:1).

Reaction Time (h)	24	48	56	96	120
Weight loss at 105 °C %	-	59.8	-	28.1	
Moisture (%)					9.2
C (%) *	58.5	49.9	57.4	55.4	61.9
H (%) *	9.6	10.1	9.9	9.0	8.6
N (%) *	1.2	-	-	1.3	1.3
S (%) *	0.7	0.3	0.5	0.7	0.9
O (%) **	30.0	39.8	32.2	33.6	27.3
HHV (kJ/kg)	28,595	24,374	28,200	26,780	29,730
LHV (kJ/kg)	26,565	-	26,110	24,870	27,950
Density (kg/dm <sup>3</sup> )	-	-	1.02 (25 °C)	-	1.41 (25 °C)

\* daf—dry ash-free basis; \*\* oxygen determined by difference; mass percentages.

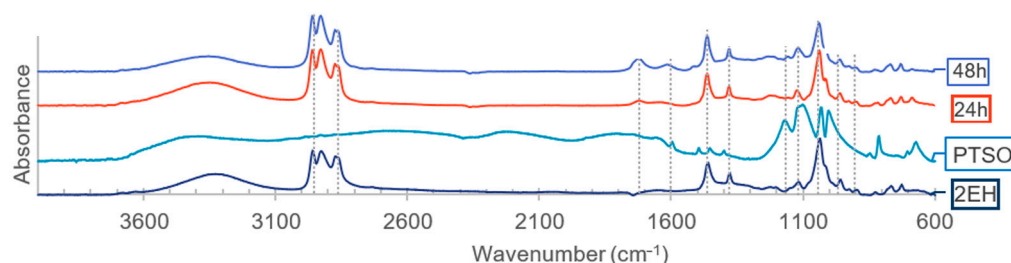
**Table 6.** Elemental analysis, weight loss at 105 °C, moisture content, calorific value, and density of the liquefied product produced in the third reaction. (Solvents: 2EH and DEG 1:1).

Reaction Time (h)	4	8	12	24	48	56
Weight loss at 105 °C % (m/m)	35.1	35.7	35.1	35.2	31.9	35.9
Moisture % (m/m)						2.1
C (%) *	62.6	62.9	62.4	62.2	60.4	60.8
H (%) *	9.0	9.1	9.5	9.4	9.0	9.3
S (%) *	0.8	0.8	0.7	0.6	0.8	0.7
O (%) **	27.6	27.2	27.5	27.8	29.9	29.3
HHV (kJ/kg)	30,282	30,364	30,551	29,933	28,530	29,108
Density (kg/dm <sup>3</sup> )	1.36	1.37	1.33	1.36	1.39	1.40

\* daf—dry ash-free basis; \*\* oxygen determined by difference; mass percentages.

### FTIR Analysis

The FTIR spectra of the bio-oils produced in different stages of the first pilot liquefaction are presented in Figure 6, alongside the spectra of the solvent and catalyst. As seen, the presence of 2EH in the liquefied products is revealed by the peaks at 2958, 2926, 2872, 1460, 1380, and 1038 cm<sup>-1</sup>. On the other hand, the intensity of the band at around 1730 cm<sup>-1</sup> increases with the reaction time. As mentioned above, this band corresponds to the presence of carboxylic groups and can be associated with compounds derived from depolymerization reactions, such as lactic acid, levulinic acid, or furfural [27,28]. Nevertheless, this peak may also indicate the presence of unreacted biomass since biomass is continuously added to the reactor. The peaks at 1590 and 1170 cm<sup>-1</sup> in the bio-oil spectra are associated with the catalyst and correspond to C=C bonds of the aromatic rings and R-SO<sub>2</sub>-OH bonds. Thus, it is possible to conclude that the catalyst was not entirely removed. The peak at 1590 cm<sup>-1</sup> may also be associated with aromatic vibrations of lignin polymers with C=O bonds. Finally, the low-intensity peaks at 766 and 726 cm<sup>-1</sup> in the solvent spectrum correspond to C-C bond vibrations.

**Figure 6.** FTIR analysis of the 2-EH, catalysts, and first liquefaction bio-oils (solvent: 2EH).

The spectrum of the bio-oils produced in one of the reactions carried out with the mixture of 2EH and DEG as solvents is presented in Figure 7 (reaction 3 in the Supporting Information) and shows that the bio-oils and polyols contain 2EH and DEG. In fact, the peaks at 2958, 2926, and 2872 cm<sup>-1</sup> due to C-H bonds are visible in both phases. On the other hand, the peak at 1350 cm<sup>-1</sup>, representing C-OH vibrations, as well as at 1215 and 1118 cm<sup>-1</sup>, is associated with the C-O bonds of esters, and the peaks at 912 and 886 cm<sup>-1</sup>, corresponding to C-O-C bonds, indicate the presence of DEG. The peak at 1038 cm<sup>-1</sup>, indicative of C-OH groups of both solvents, appears in the spectra of all samples.

The analysis of the FTIR spectra of the bio-oils and polyol samples reveals a peak at 1640 cm<sup>-1</sup>, corresponding to the C=C bonds of furfural or HMF (hydroxymethylfurfural), which result from the depolymerization reactions of cellulose and lignin [24,27]. This peak is present in the spectra of bio-oils and polyols, showing that these species were not completely extracted to the aqueous phase.

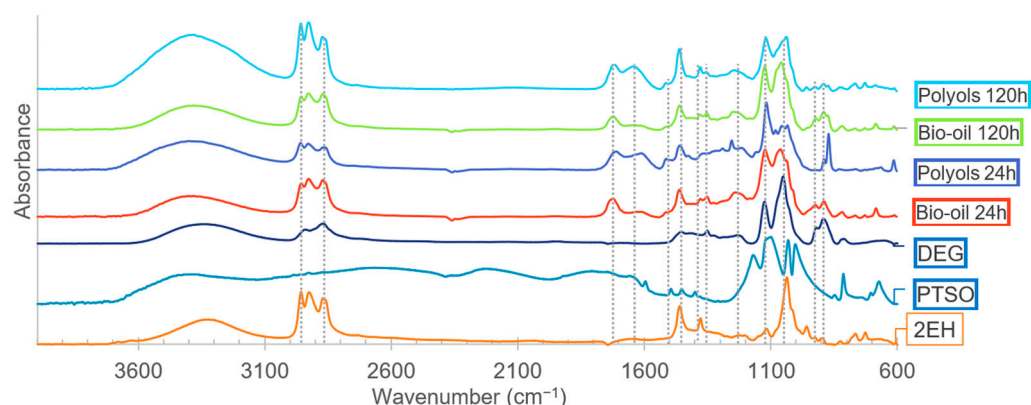


**Figure 7.** FTIR analysis of the solvents, catalysts, bio-oils, and polyols produced in the third liquefaction reaction (solvents: 2EH and DEG).

#### TG/DTG/DSC Analysis

Figure 8 presents the thermogravimetric analysis of the bio-oil produced after 56 h of the second liquefaction reaction.

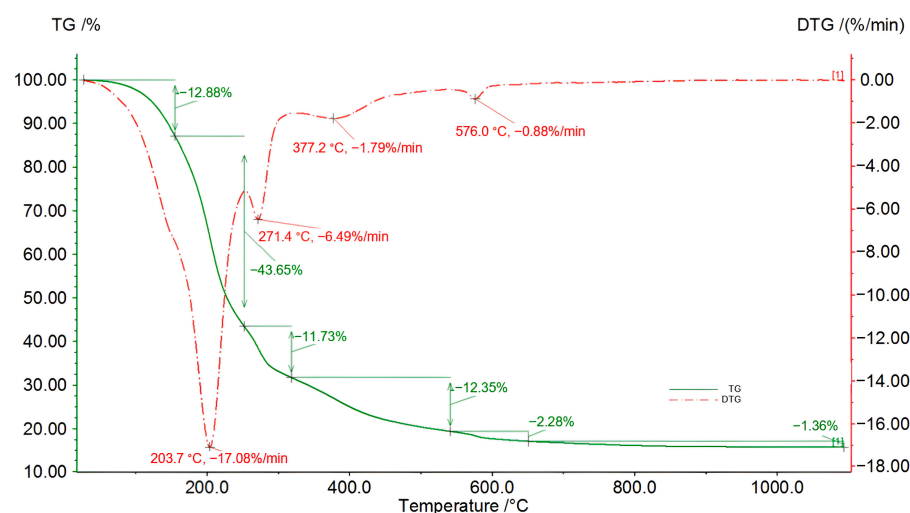


**Figure 8.** TG/DSC/DTG curves of the bio-oil produced after 56 h of the second liquefaction reaction (solvents: 2EH and DEG).

The DTG curve above shows an initial slope variation at 139.0 °C, indicating a significant mass loss of 12.9% until 207 °C. The 207–286 °C temperature interval exhibits the highest mass rate variation of approximately 45.1%, peaking at 251.4 °C, suggesting that the compounds within this temperature range are the most abundant in the liquefied product. Beyond 286 °C, the mass loss rate decreases significantly, with a further loss of 15.6% until 353 °C. The DTG curve stabilizes at this point, indicating a constant mass variation with time. The decomposition observed in this range may be attributed to the degradation of non-reacted biomass constituents, particularly lignin polymers. Lastly, a minor peak weight loss is observed at 581.9 °C, which could be associated with the degradation of more complex compounds that either did not decompose during the reaction or resulted from repolymerization reactions.

The TG curve of the 8 h product from the third reaction shown in Figure 9 exhibits a distinct pattern. In fact, five distinct plateaus in the TG and DTG curves can be distinguished. The first plateau spans from 25 to 152 °C, with a mass loss of 12.9%, and the second plateau, ranging from 152 to 253 °C, includes the most pronounced peak of mass loss at 204 °C, resulting in a loss of 43.7% of the sample mass. This temperature range corresponds to the degradation of DEG. The third plateau (253–295 °C) peaks at 271.4 °C,

indicating a further 9.7% mass loss. The last two plateaus occur between 295 and 466 °C and 466 and 603 °C, with 12.4% and 2.3% mass losses, respectively.

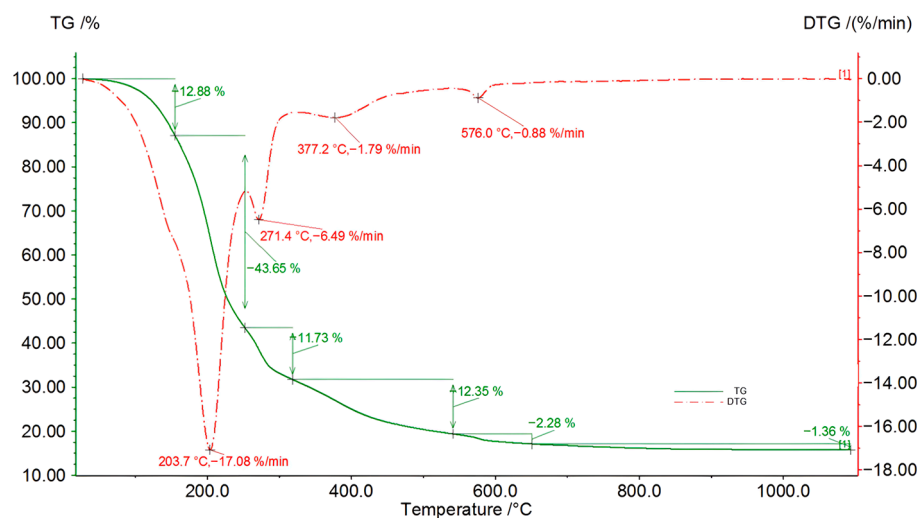


**Figure 9.** TG/DSC/DTG curves for an 8 h sample of the third liquefaction reaction (solvents: 2EH and DEG).

### 2.3.2. Characterization of the Aqueous Phases and Dried Sugars FTIR Analysis

The FTIR analysis of the aqueous phases obtained in the water extractions of the bio-oils produced in the second liquefaction after 56 h and 120 h of reaction is presented in Figure 10. As seen, both samples exhibit an elongated band at approximately  $3400\text{ cm}^{-1}$ , corresponding to moisture [29]. The peaks at  $2959$ ,  $2929$ , and  $2873\text{ cm}^{-1}$  are associated with C-H bonds, which are characteristic of the solvent 2EH. Similar peaks in the range of  $1462$  and  $1379\text{ cm}^{-1}$  are also related to C-H vibrations. The prominent peaks at  $1121$ ,  $1056$ ,  $926$ , and  $890\text{ cm}^{-1}$ , representing the C-O bonds, C-OH vibrations, and C-O-C bonds of the ester groups, match with the peaks of DEG, which is highly soluble in water.

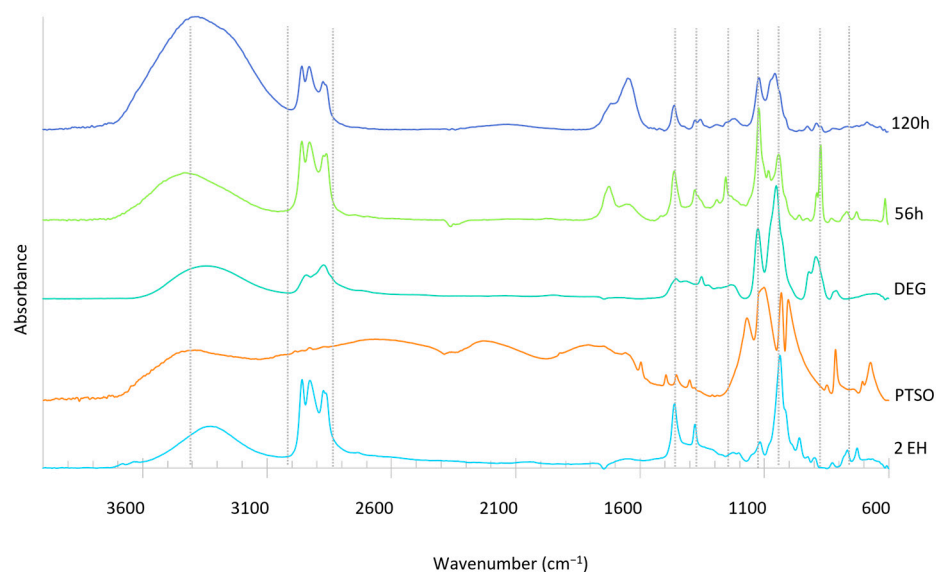


**Figure 10.** FTIR analysis of the extraction waters of the second liquefaction reaction (solvents: 2EH and DEG).

Figure 10 also shows that there are several peaks in the spectra of the aqueous phases that do not belong to the solvents. Notably, the peak at  $1648\text{ cm}^{-1}$  observed in the FTIR spectrum of the extraction water collected after 56 h of reaction corresponds to vibrations associated with the C=C bonds. Furthermore, two additional peaks were recorded at frequencies of  $1723$  and  $1235\text{ cm}^{-1}$ , which can be attributed to carboxylic groups and COOH vibrations, respectively. Thus, through comparison with the reference spectra of different sugars, it was concluded that the above-mentioned peaks are also present in the spectra of furfural, HMF (hydroxymethylfurfural), lactic acid, and levulinic acid.

Figure 11 presents the FTIR spectra of the dried sugar solutions recovered from the aqueous phases of water extraction of two bio-oils (24 h and 48 h) of the first liquefaction reaction. The spectra exhibit bands of the catalyst, specifically at  $1102$ ,  $1032$ ,  $1005$ ,  $814$ , and  $673\text{ cm}^{-1}$  of the R-SO<sub>2</sub>-OH, O=S=O, S-C, and S-O bonds. Therefore, it is possible to conclude that the catalyst is transferred to the aqueous phase during the extraction process, a hypothesis further corroborated by the acidic pH of the extraction waters (1.7 in this case). Additionally, the spectra have a band in the region of  $3300\text{ cm}^{-1}$ , indicating the presence of hydroxyl (-OH) groups associated with either moisture or alcohol. As expected, the intensity of this band decreases as the drying temperature increases from  $60\text{ }^{\circ}\text{C}$  to  $80\text{ }^{\circ}\text{C}$ .

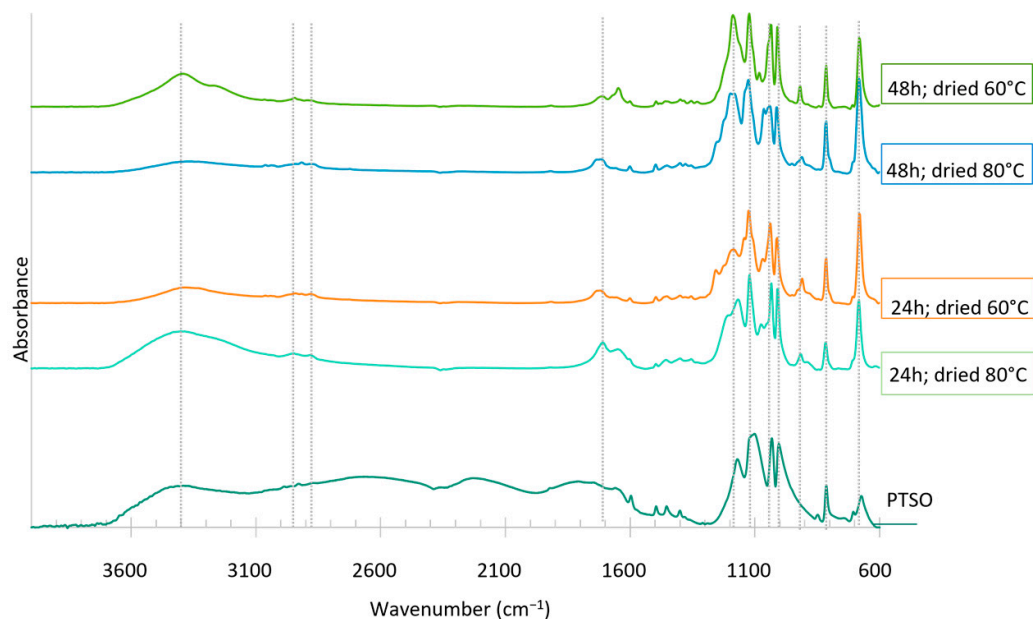


**Figure 11.** FTIR analysis of the dried sugars extracted from bio-oils produced in the first liquefaction after 24 h and 48 h of reaction (solvent: 2EH).

In the sugar sample recovered from the 24 h reaction bio-oil, two peaks at  $2931$  and  $2874\text{ cm}^{-1}$  are evident. These peaks correspond to aliphatic compounds containing carbon-hydrogen bonds. On the other hand, in the sugar dried at  $60\text{ }^{\circ}\text{C}$ , prominent peaks appear at frequencies of  $1720$  and  $1651\text{ cm}^{-1}$ , which can be attributed to carbonyl and conjugated double bonds, respectively.

#### TG/DTG/DSC Analysis

Thermogravimetry analysis of the extraction water and of the dried sugars are presented in Figures 12 and 13.

In the DTG curve of the extraction water in Figure 12, three peaks are observed at  $150.2$ ,  $196.9$ , and  $245.7\text{ }^{\circ}\text{C}$ , whereas in the dried sugars resulting from this water (Figure 13), three peaks also appear but at different temperatures of  $183.7$ ,  $259.7$ , and  $479.4\text{ }^{\circ}\text{C}$ . Probably, the first peaks in each curve, at  $150.2$  and  $183.7\text{ }^{\circ}\text{C}$ , may correspond to the same compound. In fact, the mass loss associated with water in the aqueous phase has a huge influence on this

DTG curve, overlapping with the peak at 183.7 °C. After water removal, the concentration of this component increases, showing a peak at 100 °C with an associated mass loss of 13.49%. The analysis of the DTG curves of several pure compounds that can be present in these aqueous phases (Supplementary Information) shows that furfural has a decomposition temperature close to 172.1 °C, which is similar to the temperature at which the mass loss of the analyzed sugar occurs. Although there is still a considerable difference in these peak temperatures, the color and odor of the obtained sugar solutions resemble those described for furfural, which have a yellowish liquid with a strong odor [30].

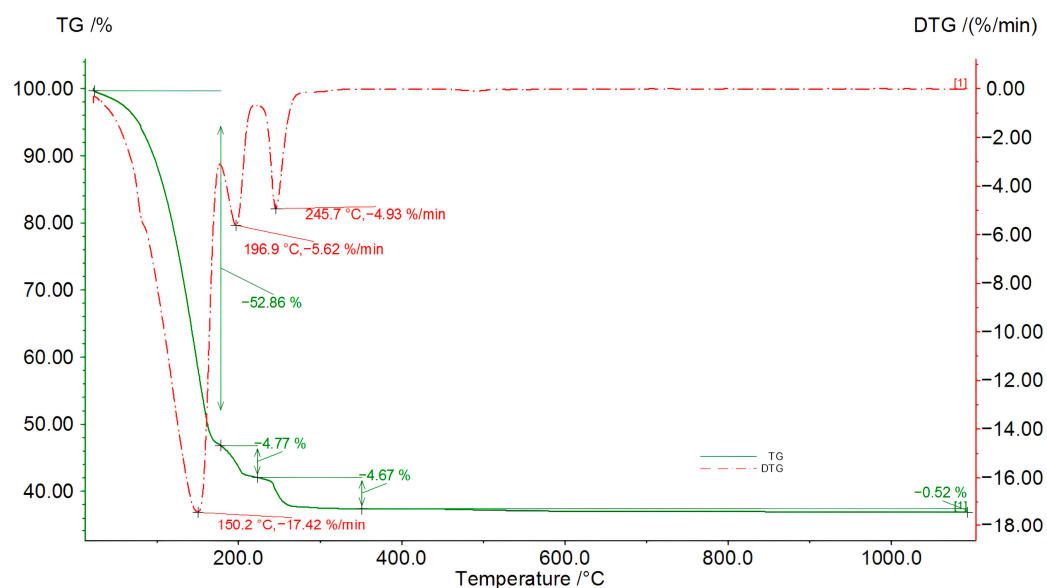


**Figure 12.** TG/DSC/DTG curves of the aqueous phase after water extraction of the bio-oil produced in the first liquefaction after 24 h of reaction (solvent: 2EH).

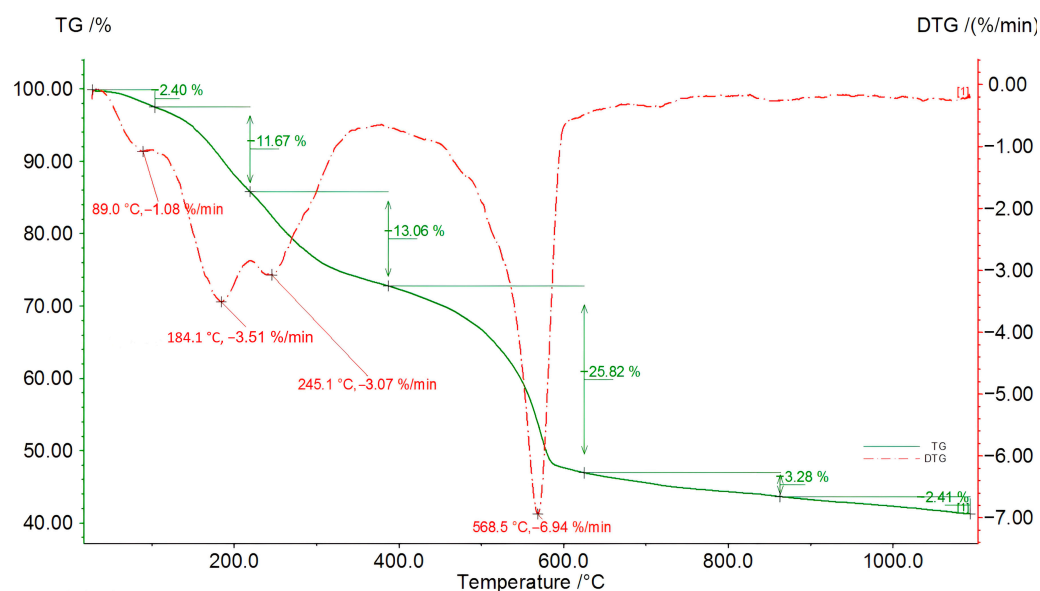


**Figure 13.** TG/DSC/DTG curves of the dried sugars recovered from the aqueous phase of water extraction of the bio-oil produced in the first liquefaction after 24 h of reaction (solvent: 2EH).

Another peak that appears in the three TG/DTG curves is the mass loss peak at around 245 °C. Comparison with the DTG curves of the standard compounds (Supplementary Information) allows us to conclude that this peak is characteristic of both levulinic acid and

lactic acid, which confirms the findings of the FTIR spectra that indicate the presence of the functional groups of these compounds.

Figure 13 presents the TG data for the aqueous phases of bio-oil water extraction and some of the sugars recovered after drying these aqueous phases.

In addition to the previously mentioned peak at 180 °C (5.0% mass loss), the sugars exhibit a peak in the range of 240–250 °C (62.7% mass loss), identified as either lactic acid or levulinic acid. This sample also has distinctive mass loss peaks, particularly at 320.5 and 581.7 °C, with mass variations of 16.1% and 2.0%, respectively. The peak at 320 °C is characteristic of glucose (Supplementary Information), which is also found in sugar dimers, such as cellobiose formed by two glucose molecules.

#### HPLC-MS/MS Analysis

HPLC MS/MS was the analytical technique used to characterize the sugars in the aqueous phase produced in bio-oil water extraction. First, the relevant standard solutions were individually injected into the mass spectrometry instrument to identify their characteristic fragmentation patterns. The collision energy was adjusted for each molecule under investigation. During the infusion process, the first quadrupole was set to the molecular mass of the corresponding standard ion, and the specific fragmentations of each identified signal (resulting from bond cleavage of lower mass ions) were determined by analyzing the molecular masses and the chemical structures after collision with argon in the collision cell. This procedure allowed us to identify the specific transitions for each standard that is essential for the HPLC analysis. The observed fragmentations were attributed to various processes including the loss of H<sub>2</sub>O, the formation of double bonds, the loss of -CH<sub>2</sub>O groups, the loss of H<sub>2</sub>, or the cleavage of bonds within aromatic rings [31–34]. Standards used in HPLC-MS/MS are shown in Table 7.

**Table 7.** Standards used in HPLC-MS/MS.

Compounds	Standard
Arabinose   Xylose   Ribose	Succinic Acid
Glucose   Sorbose   Galactose Fructose   Mannose	Levulinic Acid
Lactic Acid	Xylitol
Cellobiose   Trehalose	Rhamnose

The comparison between the standard retention times with the ones of the injected solutions allowed us to identify the main compounds in the solution. However, some of the standards with identical masses that were grouped in the mass spectrometry analysis have different retention times in the HPLC run (Supplementary Information). Nevertheless, this HPLS-MS/MS analysis revealed the presence of intense peaks of levulinic acid and the catalyst (PTSO) (Supplementary Materials).

These findings are consistent with the results obtained from the FTIR analysis.

#### 2.3.3. Characterization of the Reaction Condensates

The condensates recovered during the liquefaction reactions are expected to be formed by a mixture of the solvent/s with the water from the biomass moisture and formed during the depolymerization reactions.

#### FTIR Analysis of the Condensates

The FTIR spectra of the organic and aqueous phases obtained after phase separation of the condensates collected after 24 and 48 h of reaction in the third liquefaction are presented in Figure 14, together with the spectra of the pure solvents and lactic acid.

As seen, the spectra of the aqueous and organic phases present the same peaks. Furthermore, the peak characteristics of 2EH (2960, 2929, 2873, 1462, 1121, 1035, 826, 768, and 729 cm<sup>-1</sup>) and DEG (1215, 1121, 1035, 961, and 892 cm<sup>-1</sup>) are present in the condensates,

which confirms that part of the solvents is carried over during water evaporation. Additionally, the peaks at 1731, 1235, 1178, and 1117  $\text{cm}^{-1}$ , corresponding to C=O bonds, -COOH groups, C-O bond vibrations, and C-OH vibrations, respectively, which are attributed to carboxylic acid functional groups, are also present in the condensates but not in the solvents. In a comparison with the spectra of different compounds, it was observed that these peaks can be due to the presence of lactic acid in the condensates, which were also carried away from the reaction medium during evaporation.

The peaks at around 3374  $\text{cm}^{-1}$ , corresponding to OH groups, are very important in the aqueous phase of the condensates of the 48 h reaction sample. Furthermore, the peak at 1640  $\text{cm}^{-1}$ , typically associated with C=C vibrations, is also present, and can be attributed to the presence of furfural and HMF.

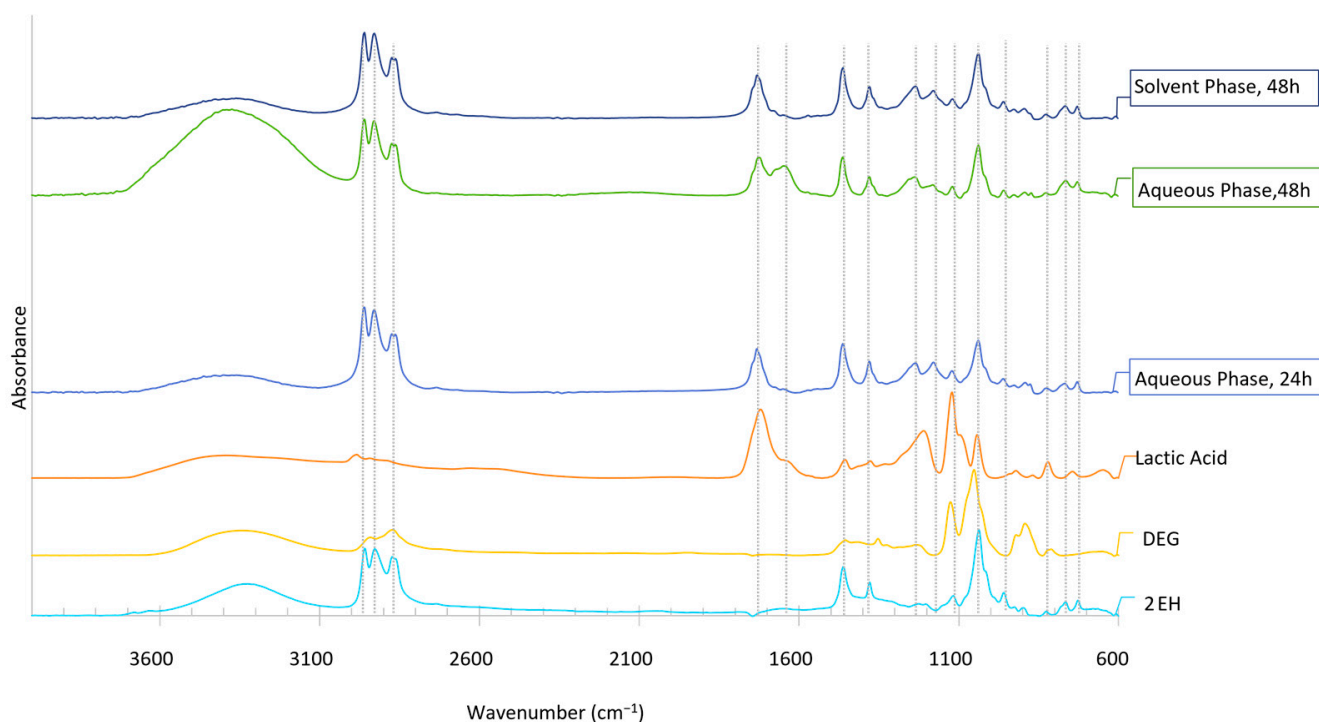


**Figure 14.** FTIR spectrum of the third liquefaction condensates.

Bearing in mind the previous results, it is possible to conclude that the evaporation of the water, produced by the depolymerization reactions and by biomass dehumidification, carries some solvent. Moreover, the acidic pH of the condensed aqueous phase can be due to the presence of carboxylic acids and/or some catalysts. Finally, the FTIR spectra of the condensate aqueous phases indicate that some of the products of the depolymerization reactions, like lactic acid, levulinic acid, and furfural, are also removed from the reaction medium to the condensates.

#### 2.3.4. Bio-Oil Aging

One factor that can hinder the widespread use of biofuels in industrial applications is their tendency to degrade over time during storage. To study the effect of the storage time on the properties of these bio-oils, a sample of the bio-oil produced in the third liquefaction after 10 h of reaction was used. The aging process was accelerated by subjecting the biofuel sample to a temperature of 80 °C, following the method described by Udomsap et al. [35].

Three bio-oil samples were put in an oven at 80 °C for 1, 2, and 7 days. After the specified aging period, the samples were removed from the oven and cooled. The density was measured after cooling, and it was not possible to measure the viscosity because the samples were solid at room temperature.

It is worth noting that according to Oasmaa et al. [36], the changes observed after 24 h at 80 °C are equivalent to the changes that would occur if the biofuel is kept at room temperature for one year [36].

The density measurements of the fresh and aged bio-oils are presented in Figure 15. As expected, the density of the bio-oils increases with the storage time [37] and follows a linear relation ( $R^2 = 0.99$ ). This density increase can be attributed to the occurrence of repolymerization reactions due to the presence of free radicals in the biofuel. These radical reactions form compounds with larger molecular weight, thereby increasing the overall density of the biofuel.

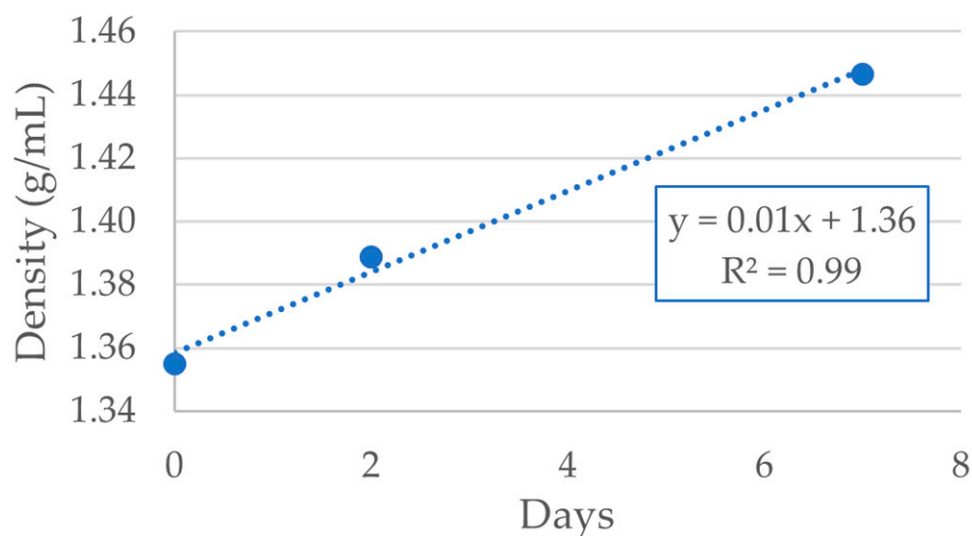


**Figure 15.** Evolution of bio-oil density with time (third reaction, 10 h).

One of the alternatives to minimize biofuel degradation during storage is the addition of a solvent that can easily undergo dehydrogenation reactions, as the released hydrogen atoms will react rapidly with the free radicals, hindering the repolymerization reactions responsible for bio-oil degradation [37].

### 3. Experimental

#### 3.1. Liquefaction

The biomass samples used in this work are *E. globulus* bark and *E. globulus* sawdust supplied by the Navigator Company. The optimum liquefaction conditions were studied elsewhere [4,14]. Diethylene glycol (DEG) from Sapec, 2-Ethylhexanol (2EH) from Brenntag, and the previously produced bio-oil were used as solvents; p-Toluenesulfonic acid was the catalyst. The liquefaction experiments described in this work were carried out at a laboratory scale in a 2 L batch reactor, and at a pilot scale in a 3-tonne pilot reactor installed within the ENERGREEN project. Before all experiments, the biomass was pre-treated by contact with part of the solvent (typically  $\approx 2$  mL of solvent/100 g of biomass at 80 °C for 60 min). In the pilot scale tests, this pre-treatment is carried out inside the screw conveyor that transports the biomass to the reactor, and this stage also takes around 60 min. This pre-treatment promotes the swelling of the cells, allowing better access to the catalyst to the biomass components [4].

The conditions used in the laboratory tests with *E. globulus* bark and sawdust are presented in Table 8. To start each experiment, the solvent quantity was added to the reactor, the thermostat was set to 80 °C, and the stirrer was switched on and set at a speed of around 180 rpm. When the temperature reached 80 °C, the pre-treated biomass was added to the reactor and the thermostat was set at 160 °C. During the temperature rise, at around 99 °C, a mixture of water and solvent, which form an azeotrope (40% water and 60% solvent,  $w:w$ ), was collected in a dean stark. After its complete removal, the temperature

continues rising until the defined set point. When the reactor mixture reached 160 °C, the desired quantity of the catalyst was added to the reactor, and the reaction timer was set to begin. After the reaction, acetone was mixed with the reactor content, and the mixture was filtered to separate the solids. The filtrate was distilled to remove the acetone and recover the bio-oil. The solid residues were washed with acetone and dried at 80 °C in an oven and then cooled down to room temperature in a desiccator and weighed. The weight of the residue was used to calculate the conversion of the biomass into bio-oil using the following equation:

$$\%C = \frac{(W_i - W_f)}{W_i} \times 100 \quad (1)$$

where  $W_i$  and  $W_f$  are, respectively, the initial and final mass of solids.

In the laboratory tests carried out using sequential biomass additions, the solvent and the catalyst were added initially to the reactor and heated while stirring. When the reaction temperature was reached, 10% wt of biomass vs. the solvent was added to the reactor. This biomass addition was repeated hourly until the limit condition, which corresponds to the formation of a very viscous mixture impossible to stir and filtrate.

The procedure used in the pilot reactor is presented in EP3689847, which describes a catalytic and continuous thermochemical process of biomass liquefaction to produce biofuel and valuable products. In this process, the biomass is transported to the reactor through a screw conveyor where, as mentioned above, the solvent or the mixture of solvents is injected to promote the swelling of the biomass cells. Simultaneously, the preheating of the mixture is carried out through the counter-current passage of the vapors removed from the reactor. Liquefaction was carried out at atmospheric pressure and 160 °C. The biomass incrementation was 10% mass per hour.

**Table 8.** Experimental conditions used in the lab-scale liquefaction of *E. globulus* bark and *E. globulus* sawdust.

Conditions	<i>E. globulus</i> Bark	<i>E. globulus</i> Sawdust
Weight loss at 105 °C (%)	53.4	44.4
Ash (%)	5.1	1.7
Biomass (%)	10	10
Catalyst (%)	1.5	1.5
2EH (g)	750	750
Biomass (g)	188.3	152.4
Temperature (°C)	160	160
Pressure (atm)	1	1
Reaction time (h)	1	1

Note: %—mass percentages.

The experimental conditions employed in the pilot scale reactor were designed to replicate the conditions used in the laboratory experiments. Thus, *E. globulus* sawdust was selected as biomass, and a concentration of 1.5% p-toluenesulfonic acid, relative to the amount of biomass, was used. In the first liquefaction reaction, only 2EH was employed as a solvent. However, in the subsequent two liquefaction reactions, a mixture of 2EH and DEG in a 1:1 mass ratio was utilized. In this pilot scale reactor, the liquefaction process occurs in a semi-continuous mode according to the simplified flowsheet presented in Figure 16. After liquefaction, the sugars produced by the decomposition of the lignocellulosic chains were extracted with water. After phase separation, it was possible to obtain an aqueous phase that is rich in several valuable compounds and an organic phase, called polyols, that, after drying, is a valuable biofuel.

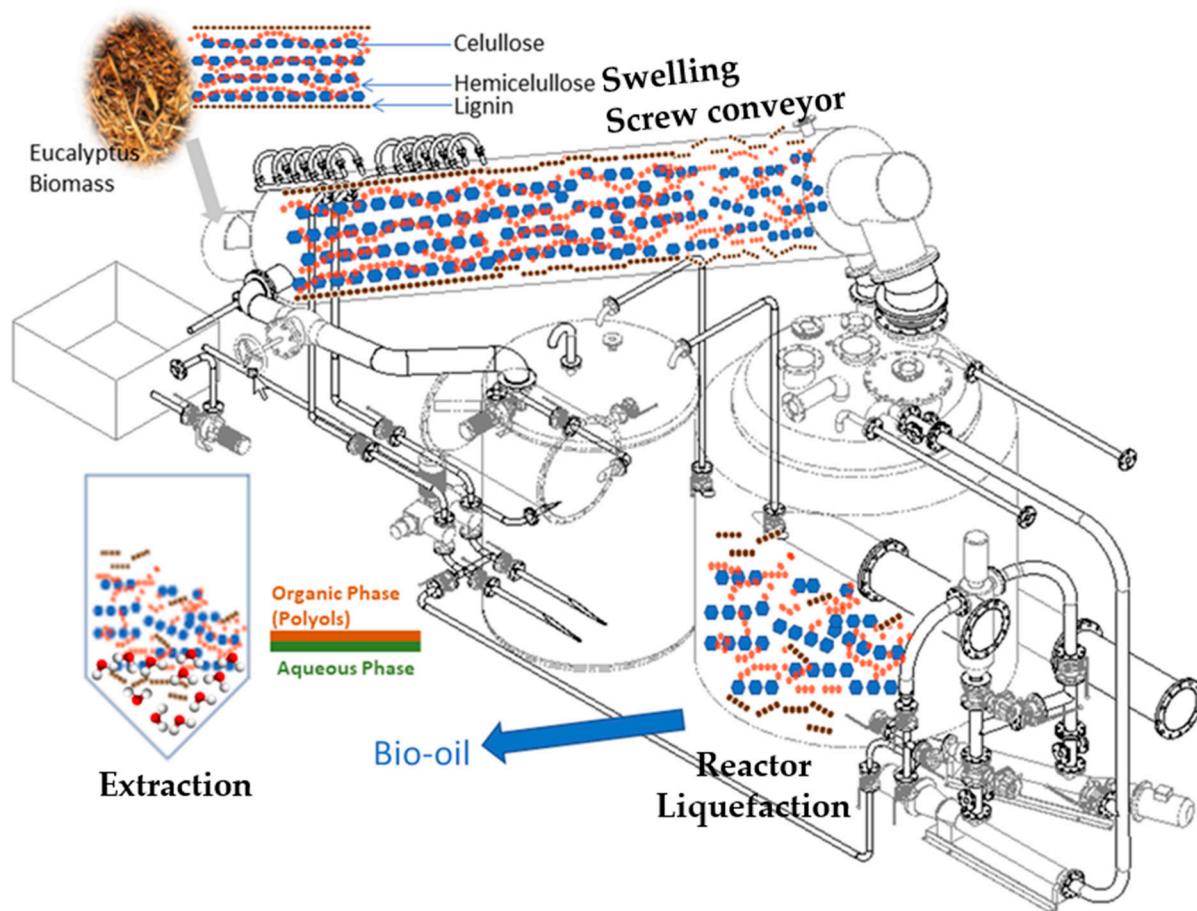


**Figure 16.** Flowsheet of the biomass liquefaction process and sugar extraction stage (polyols: hydrophobic compounds (blue and orange chains); aqueous phase (water and hydrophilic compounds (brown chains)).

### 3.2. Sugar Extraction

In the laboratory tests, the extraction of sugars from the bio-oils was carried out with distilled water or the condensates recovered from the same liquefaction batch. After the addition of the water/condensates in the proportion of 1:1 (weight) vs. the bio-oil, the mixture was stirred slowly with a magnetic stirrer for 1 h and placed in a separating funnel overnight. After phase separation, the heavier yellowish aqueous phase was collected for analysis, and the organic phase was weighed, dried, and analyzed [12].

The aqueous phase after water extraction was further processed to determine its sugar content. Therefore, after vacuum filtration, a portion of the filtered solution is weighted and dried. To avoid sugar degradation and caramelization during water evaporation, the oven was kept at 60 °C. The sugar crystals were collected and weighed, and the sugar content in the aqueous phase was determined using Equation (2), where the mass of the water refers to the initial mass of the water used in the extraction step.

$$\text{Sugar content (\%)} = \frac{\text{Mass of Sugar crystals}}{\text{Mass of water}} \times 100 \quad (2)$$

### 3.3. Characterization Techniques

Several analytical techniques were used to characterize the biomass and the liquefied products using standards of cellulose, hemicellulose, and lignin. Thermogravimetric analysis (TGA- STA 449 F5 Jupiter equipment coupled with Proteus Analysis 6.1.0 software of NESTZSCH), elemental analysis, and mid-infrared Fourier-transform spectroscopy (FTIR-ATR BOMEM FTLA2000-100, ABB CANADA (Edmonton, AB, Canada) in

the 4000–400  $\text{cm}^{-1}$  range) were used. TGA was used to determine the weight loss at 105 °C of the bio-oils, whereas the water content of some of the samples was determined using the Karl–Fisher method. HPLC-MS (high-performance liquid chromatography with mass spectroscopy), which allows the analysis of polar compounds with high molecular weights, was also used.

The HPLC-MS/MS system comprised a Waters HPLC chromatography unit (Alliance 2695, Waters, Manchester, UK) and a Micromass Triple Quadrupole Mass Spectrometer (Quattro Micro, Waters, Manchester, UK), connected to a nitrogen generator (1800 L/h, 99% purity). For collision-induced dissociation experiments, 99.999% argon (Alphagaz, Argon 1, B10, Air Liquide Portugal, Algés, Portugal) was used at a pressure of 3.5 psi. The chromatographic separation employed two columns in series: a pre-column XBridge BEH Amide 2.5  $\mu\text{m}$  XP VanGuard Cartridge 2.1 mm  $\times$  5 mm and a column XBridge BEH Amide 2.5  $\mu\text{m}$ , 2.1 mm  $\times$  150 mm, both from Waters Corporation, maintained at 25 °C. The isocratic method used a mobile phase consisting of 95% MeOH with 10 mM ammonium acetate and 5% of a MeOH (80%):H<sub>2</sub>O (20%) solution. The eluent flowed at 0.2 mL/min throughout the run. Each run utilized a 10  $\mu\text{L}$  sample injection, with samples kept at 20 °C. Detection in the ESI-MS/MS detector was performed in the negative mode. The following mass spectrometry detector parameters were optimized and consistently used: capillary at 3 kV, extractor at 3 V, Rf lenses at 0.5 V, source temperature at 140 °C, desolvation temperature at 220 °C, desolvation gas flow at 600 L/h, cone gas flow at 60 L/h, and cone voltage at 20 V or 50 V, depending on the compound being analyzed. All mass transitions were optimized in previous direct infusion experiments using solutions with a concentration of 0.5  $\mu\text{g/mL}$ .

#### 4. Conclusions

This work presents a comparative study of the use of *E. globulus* sawdust and bark as biomass feedstock for biofuel production. In what concerns feedstock characterization, TG analysis allowed us to estimate the relative composition in the three biopolymers of the two biomasses, and the composition of the two biomasses anticipates easier liquefaction of sawdust due to its higher hemicellulose and lower lignin contents.

In the laboratory-scale liquefaction experiments of bark and sawdust, the conversion of the biomass into bio-oil was greater than 90%. Nevertheless, a highly viscous liquid was produced after 6 or 7 incremental additions of biomass, respectively. In the industrial scale experiments, the biomass was completely liquefied, and the density of the bio-oil at 25 °C also increased from 1.02  $\text{kg/dm}^3$  after 56 h of reaction to 1.45  $\text{kg/m}^3$  for the 120 h sample.

The liquefaction products have higher calorific values ( $\approx 33$  MJ/kg for the lab liquefactions and  $\approx 27$ –30 MJ/kg for the industrial ones) than the original biomasses ( $\approx 18$  MJ/kg).

The FTIR spectra of the bio-oils produced in the various liquefaction reactions at lab and pilot scales revealed the presence of compounds derived from biomass depolymerization, such as lactic acid, levulinic acid, and furfural. The presence of unreacted biomass and the catalyst was also detected. HPLC-MS/MS analysis validated the presence of levulinic acid and a catalyst (PTSO) in the aqueous phase obtained in bio-oil water extraction.

Finally, the study of bio-oil aging showed an increase in bio-oil density with storage time (density ( $\text{kg/dm}^3$ ) =  $0.01 \times \text{time}(\text{days}) + 1.36$ ), which can be attributed to repolymerization reactions mediated by free radicals. Therefore, it is possible to conclude that storage conditions and duration significantly influence the properties and quality of the biofuel.

In conclusion, the results obtained in this work allow us to conclude that *E. globulus* is a promising feedstock for sustainable biofuel production and biorefinery.

#### 5. Patents

EP 3689847—Ângela Nunes, João Bordado, Joana Neiva Correia, Margarida Mateus, Flávio Oliveira, and Rui Lopes, catalytic and continuous thermochemical process of production of valuable derivatives from organic materials and waste, 2018.

**Supplementary Materials:** The following supporting information can be downloaded at <https://www.mdpi.com/article/10.3390/catal13101379/s1>. Figure S1. FTIR Spectrum of Sugars Standards. Figure S2. TG/DTG/DSC of glucose; Figure S3. Curva de TG/DTG/DSC of furfural; Figure S4. TG/DTG/DSC of lactic acid; Figure S5. TG/DTG/DSC of Levullinic acid; Figure S6. TG/DTG/DSC of cellobiose; Figure S7. TG/DTG/DSC of Succinic Acid; Figure S8. Mass spectrum of the sugar solution from the third reaction by direct infusion: cone 20V (left) and 50V (right); Figure S9. HPLC Chromatogram for all standards sugars (TIC—Total Ion Count).

**Author Contributions:** Methodology, I.F., M.J.N.C. and M.M.; Validation, M.J.N.C., J.B., D.M.C. and M.M.; Formal analysis, I.F. and J.C.; Investigation, I.F. and M.J.N.C.; Data curation, J.C.; Writing—original draft, M.J.N.C., D.M.C. and M.M.; Supervision, M.J.N.C.; Project administration, M.M. All authors have read and agreed to the published version of the manuscript.

**Funding:** D.M. Cecílio and M. Mateus acknowledge the funding support of the P2020 Clean Cement Line project (LISBOA-01-0247-FEDER-027500).

**Conflicts of Interest:** The authors declare no conflict of interest.

## References

1. IEA. *Global Energy & CO2 Status Report 2019*; IEA: Paris, France, 2019.
2. McKendry, P. Energy Production from Biomass (Part 2): Conversion Technologies. *Bioresour. Technol.* **2002**, *83*, 47–54. [[CrossRef](#)]
3. Bridgwater, T. Biomass for Energy. *J. Sci. Food Agric.* **2006**, *86*, 1755–1768. [[CrossRef](#)]
4. Braz, A.; Mateus, M.M.; dos Santos, R.G.; Machado, R.; Bordado, J.M.; Correia, M.J.N. Modelling of Pine Wood Sawdust Thermochemical Liquefaction. *Biomass Bioenergy* **2019**, *120*, 200–210. [[CrossRef](#)]
5. Aysu, T.; Küçük, M.M. Biomass Pyrolysis in a Fixed-Bed Reactor: Effects of Pyrolysis Parameters on Product Yields and Characterization of Products. *Energy* **2014**, *64*, 1002–1025. [[CrossRef](#)]
6. González-García, P. Activated Carbon from Lignocellulosics Precursors: A Review of the Synthesis Methods, Characterization Techniques and Applications. *Renew. Sustain. Energy Rev.* **2018**, *82*, 1393–1414. [[CrossRef](#)]
7. Zhang, L.; Xu, C.; Champagne, P. Overview of Recent Advances in Thermo-Chemical Conversion of Biomass. *Energy Convers. Manag.* **2010**, *51*, 969–982. [[CrossRef](#)]
8. Xu, F.; Yu, J.; Tesso, T.; Dowell, F.; Wang, D. Qualitative and Quantitative Analysis of Lignocellulosic Biomass Using Infrared Techniques: A Mini-Review. *Appl. Energy* **2013**, *104*, 801–809. [[CrossRef](#)]
9. Cecílio, D.M.; Gonçalves, J.R.M.; Correia, M.J.N.; Mateus, M.M. Aspen Plus® Modeling and Simulation of an Industrial Biomass Direct Liquefaction Process. *Fuels* **2023**, *4*, 221–242. [[CrossRef](#)]
10. Fernandes, F.; Matos, S.; Gaspar, D.; Silva, L.; Paulo, I.; Vieira, S.; CR Pinto, P.; Bordado, J.; Galhano dos Santos, R. Boosting the Higher Heating Value of Eucalyptus Globulus via Thermochemical Liquefaction. *Sustainability* **2021**, *13*, 3717. [[CrossRef](#)]
11. Paulo, I.; Costa, L.; Rodrigues, A.; Orišková, S.; Matos, S.; Gonçalves, D.; Gonçalves, A.R.; Silva, L.; Vieira, S.; Bordado, J.C.; et al. Acid-Catalyzed Liquefaction of Biomasses from Poplar Clones for Short Rotation Coppice Cultivations. *Molecules* **2022**, *27*, 304. [[CrossRef](#)]
12. Silva, L.; Orišková, S.; Gonçalves, D.; Paulo, I.; Condeço, J.; Monteiro, M.; Xavier, N.M.; Rauter, A.P.; Bordado, J.M.; Galhano dos Santos, R. Quantification of Hydrolytic Sugars from Eucalyptus Globulus Bio-Oil Aqueous Solution after Thermochemical Liquefaction. *Forests* **2023**, *14*, 799. [[CrossRef](#)]
13. Pan, H. Synthesis of Polymers from Organic Solvent Liquefied Biomass: A Review. *Renew. Sustain. Energy Rev.* **2011**, *15*, 3454–3463. [[CrossRef](#)]
14. Condeço, J.A.D.; Hariharakrishnan, S.; Ofili, O.M.; Mateus, M.M.; Bordado, J.M.; Correia, M.J.N. Energetic Valorisation of Agricultural Residues by Solvent-Based Liquefaction. *Biomass Bioenergy* **2021**, *147*, 106003. [[CrossRef](#)]
15. Behrendt, F.; Neubauer, Y.; Oevermann, M.; Wilmes, B.; Zobel, N. Direct Liquefaction of Biomass. *Chem. Eng. Technol.* **2008**, *31*, 667–677. [[CrossRef](#)]
16. Lu, Y.; Li, G.-S.; Lu, Y.-C.; Fan, X.; Wei, X.-Y. Analytical Strategies Involved in the Detailed Componential Characterization of Biooil Produced from Lignocellulosic Biomass. *Int. J. Anal. Chem.* **2017**, *2017*, e9298523. [[CrossRef](#)]
17. Jiang, W.; Kumar, A.; Adamopoulos, S. Liquefaction of Lignocellulosic Materials and Its Applications in Wood Adhesives—A Review. *Ind. Crops Prod.* **2018**, *124*, 325–342. [[CrossRef](#)]
18. Zhong, C.; Wei, X. A Comparative Experimental Study on the Liquefaction of Wood. *Energy* **2004**, *29*, 1731–1741. [[CrossRef](#)]
19. Zhang, W.; Liu, H.; Ul Hai, I.; Neubauer, Y.; Schröder, P.; Oldenburg, H.; Seilkopf, A.; Kölling, A. Gas Cleaning Strategies for Biomass Gasification Product Gas. *Int. J. Low-Carbon Technol.* **2012**, *7*, 69–74. [[CrossRef](#)]
20. Li, Y.; Luo, X.; Hu, S. Lignocellulosic Biomass-Based Polyols for Polyurethane Applications. In *Bio-Based Polyols and Polyurethanes*; Li, Y., Luo, X., Hu, S., Eds.; Springer Briefs in Molecular Science; Springer International Publishing: Cham, Switzerland, 2015; pp. 45–64, ISBN 978-3-319-21539-6.

21. Raspolli Galletti, A.M.; D'Alessio, A.; Licursi, D.; Antonetti, C.; Valentini, G.; Galia, A.; Nasso, N. Midinfrared FT-IR as a Tool for Monitoring Herbaceous Biomass Composition and Its Conversion to Furfural. *J. Spectrosc.* **2015**, *2015*, e719042. [[CrossRef](#)]
22. Amândio, M.S.T.; Rocha, J.M.S.; Xavier, A.M.R.B. Enzymatic Hydrolysis Strategies for Cellulosic Sugars Production to Obtain Bioethanol from Eucalyptus Globulus Bark. *Fermentation* **2023**, *9*, 241. [[CrossRef](#)]
23. Liu, Y.; Shi, H.; Wang, Y.; Wen, J. Analysis of Chemical Components and Liquefaction Process of Eucalyptus Globulus Bark. *Appl. Chem. Eng.* **2021**, *4*, 29–36. [[CrossRef](#)]
24. Knez, Ž.; Hrnčič, M.K.; Čolnik, M.; Škerget, M. Chemicals and Value Added Compounds from Biomass Using Sub- and Supercritical Water. *J. Supercrit. Fluids* **2018**, *133*, 591–602. [[CrossRef](#)]
25. De Bhowmick, G.; Sarmah, A.K.; Sen, R. Lignocellulosic Biorefinery as a Model for Sustainable Development of Biofuels and Value Added Products. *Bioresour. Technol.* **2018**, *247*, 1144–1154. [[CrossRef](#)] [[PubMed](#)]
26. Fernandes, A.; Cruz-Lopes, L.; Dulyanska, Y.; Domingos, I.; Ferreira, J.; Evtuguin, D.; Esteves, B. Eco Valorization of Eucalyptus Globulus Bark and Branches through Liquefaction. *Appl. Sci.* **2022**, *12*, 3775. [[CrossRef](#)]
27. Zhou, C.-H.; Xia, X.; Lin, C.-X.; Tong, D.-S.; Beltramini, J. Catalytic Conversion of Lignocellulosic Biomass to Fine Chemicals and Fuels. *Chem. Soc. Rev.* **2011**, *40*, 5588–5617. [[CrossRef](#)]
28. Grilc, M.; Likožar, B.; Levec, J. Hydrotreatment of Solvolytically Liquefied Lignocellulosic Biomass over NiMo/Al<sub>2</sub>O<sub>3</sub> Catalyst: Reaction Mechanism, Hydrodeoxygenation Kinetics and Mass Transfer Model Based on FTIR. *Biomass Bioenergy* **2014**, *63*, 300–312. [[CrossRef](#)]
29. Water Absorption Spectrum. Available online: [https://water.lsbu.ac.uk/water/water\\_vibrational\\_spectrum.html](https://water.lsbu.ac.uk/water/water_vibrational_spectrum.html) (accessed on 14 July 2023).
30. ICSC 0276—FURFURAL. Available online: [http://www.ilo.org/dyn/icsc/showcard.display?p\\_version=2&p\\_card\\_id=0276](http://www.ilo.org/dyn/icsc/showcard.display?p_version=2&p_card_id=0276) (accessed on 14 July 2023).
31. Demarque, D.P.; Crotti, A.E.M.; Vessecchi, R.; Lopes, J.L.C.; Lopes, N.P. Fragmentation Reactions Using Electrospray Ionization Mass Spectrometry: An Important Tool for the Structural Elucidation and Characterization of Synthetic and Natural Products. *Nat. Prod. Rep.* **2016**, *33*, 432–455. [[CrossRef](#)]
32. Taylor, V.F.; March, R.E.; Longerich, H.P.; Stadey, C.J. A Mass Spectrometric Study of Glucose, Sucrose, and Fructose Using an Inductively Coupled Plasma and Electrospray Ionization. *Int. J. Mass Spectrom.* **2005**, *243*, 71–84. [[CrossRef](#)]
33. Konda, C. Structural Analysis of Carbohydrates by Mass Spectrometry. Ph.D. Thesis, University of Purdue, Lafayette, IN, USA, 2013.
34. Haider Shipar, M.A. Formation of Methyl Glyoxal in Dihydroxyacetone and Glycine Maillard Reaction: A Computational Study. *Food Chem.* **2006**, *98*, 395–402. [[CrossRef](#)]
35. Udomsap, P.; Yeinn, Y.H.; Hui, J.T.H.; Yoosuk, B.; Yusuf, S.B.; Sukkasi, S. Towards Stabilization of Bio-Oil by Addition of Antioxidants and Solvents, and Emulsification with Conventional Hydrocarbon Fuels. In Proceedings of the 2011 International Conference & Utility Exhibition on Power and Energy Systems: Issues and Prospects for Asia (ICUE), Pattaya, Thailand, 28–30 September 2011; pp. 1–5.
36. Oasmaa, A.; Kuoppala, E. Fast Pyrolysis of Forestry Residue 3. Storage Stability of Liquid Fuel. *Energy Fuels* **2003**, *17*, 1075–1084. [[CrossRef](#)]
37. Adjaye, J.D.; Sharma, R.K.; Bakshsi, N.N. Characterization and Stability Analysis of Wood-Derived Bio-Oil. *Fuel Process. Technol.* **1992**, *31*, 241–256. [[CrossRef](#)]

**Disclaimer/Publisher's Note:** The statements, opinions and data contained in all publications are solely those of the individual author(s) and contributor(s) and not of MDPI and/or the editor(s). MDPI and/or the editor(s) disclaim responsibility for any injury to people or property resulting from any ideas, methods, instructions or products referred to in the content.